Supporting Information

Single-cell multi-element analysis reveals element distribution pattern in human sperm

Xiangwei Tian [a, b, c], Xun Li [d], Nian Liu [e], Wenbin Cui [f], Lingna Zheng [g], Yingying Guo [a, b], Yanwei Liu [a, b], Ligang Hu [b], Meng Wang [g, *], Yong Liang [h], Yongguang Yin [a, b, c, e, *], Yong Cai [a, b, i], Guibin Jiang [b], Lei Jin [d, *]

[a] Laboratory of Environmental Nanotechnology and Health Effect, Research Center for Eco-Environmental Sciences, Chinese Academy of Sciences, Beijing 100085, China

[b] State Key Laboratory of Environmental Chemistry and Ecotoxicology, Research Center for Eco-Environmental Sciences, Chinese Academy of Sciences, Beijing 100085, China

[c] University of Chinese Academy of Sciences, Beijing 100049, China

[d] Reproductive Medicine Center, Tongji Hospital, Tongji Medical College, Huazhong University of Science and Technology, Wuhan 430030, China.

[e] Institute of Environment and Health, Hangzhou Institute for Advanced Study, UCAS, Hangzhou 310024, China

[f] R&D Center, Shandong Yingsheng Biotechnology Co., Ltd., Beijing 100088, China

[g] CAS Key Laboratory for Biomedical Effects of Nanomaterials and Nanosafety, Institute of High Energy Physics, Chinese Academy of Sciences, Beijing 100049, China

[h] Hubei Key Laboratory of Environmental and Health Effects of Persistent Toxic Substances, School of Environment and Health, Jianghan University, Wuhan 430056, China

[i] Department of Chemistry and Biochemistry, Florida International University, Miami, Florida 33199, United States

*Corresponding author: Yongguang Yin (ygyin@rcees.ac.cn), Meng Wang (wangmeng@ihep.ac.cn), and Lei Jin (leijintongjih@qq.com)

Text S1 Materials, reagents, and semen treatments

One hundred and fifty-six human semen samples were collected at the Reproductive Medicine Center of Tongji Hospital (Wuhan, Hubei, China). This study was performed under the approval of the ethics committee of Tongji Hospital (No. S175), following the Good Clinical Practice and Declaration of Helsinki. Informed consents were obtained from all the participants. Semen samples were obtained by masturbation, followed by 30 minutes of liquefaction and analysis of the physicochemical properties and semen quality according to the World Health Organization guideline.[1] The semen samples were classified into high- and low-quality groups based on their semen quality parameters according to previously established criteria.[2] An appropriate amount (~0.8 mL) of the remaining semen was taken from each sample and separately placed in sterile and metal-free cryogenic vials (Corning; Jiangsu, China). After mixing thoroughly with equal amounts of sterile sperm freezing medium (CooperSurgical; Trumbull, CT, USA), the samples were placed in liquid nitrogen to be frozen. The samples were transported using dry ice to maintain a low temperature of -78.5 °C before being stored in a -80 °C refrigerator. It was demonstrated by microscopic observation that frozen-thawed sperm cells still maintained their full morphology and good viability (Fig. S2).

Metal-free 15-mL polypropylene (PP) centrifuge tubes were purchased from Corning (Jiangsu, China). All the glass bottles were first soaked in 30% HNO_3 for at least 24 h, and then rinsed with ultrapure water (UPW) in triplicate. 4-(2-Hydroxyethyl)piperazine-1-ethanesulfonic acid (HEPES) was purchased from J&K Chemicals (Beijing, China). A stock solution of HEPES was prepared by dissolving solid HEPES (0.2 M) in UPW. NaCl, NaOH, and H_2O_2 (30%) were all guaranteed reagents and purchased from Sinopharm Chemical Reagent (Shanghai, China). Isotonic HEPES buffer (10 mM) was diluted from the stock solution by UPW with the addition of 0.9% (*w*/*v*) NaCl, followed by adjustment of pH to 7.2–7.4 with 0.1 M NaOH solution. Paraformaldehyde (PFA) was purchased from Macklin (Shanghai, China). PFA was first dissolved and diluted by UPW. Then, appropriate amounts of HEPES stock solution and NaCl were added, resulting in 4% (*w*/*v*) PFA isotonic solution (in 10 mM HEPES buffer) for cell fixation. Multi-element standard solution and internal standard solution (see details in Text S3) were purchased from Agilent Technologies (Santa Clara, CA, USA). An additional P standard solution was purchased from National Center of Analysis and Testing for Nonferrous Metals and Electronic Materials (Beijing, China). The Agilent multi-element standard solution and P standard solution were mixed, resulting in all the elements at a concentration of 1 mg L^{-1} for later use. All the multi-element standard solutions mentioned below refer to the mixed one. Concentrated HNO_3 (65%, *w*/*v*) was purchased from Merck (Darmstadt, Germany). A suspension of 40 nm Au nanoparticles was purchased from STREM (Newburyport, MA, USA). $HAuCl_4 \cdot 3H_2O$ used for preparing the dissolving Au standard solution was purchased from Alfa Aesar (Tianjin, China). The UPW (18.2 mΩ cm) used throughout this study was purified by a Milli-Q IQ7000 system (Millipore; Boston, MA, USA). All the reagents are analytical grade or above unless otherwise specified.

Text S2 Methods for ICP-MS analysis

Single-cell analysis of sperm cells by scICP-TOF-MS

The analytical procedures are illustrated in Fig. S1A. Semen frozen at -80 °C was thawed at room temperature (25–35 °C) for 30 min to resuscitate the sperm cells, then repeatedly blown using pipettes for thorough mixing. Samples of 1 mL of semen were taken into metal-free PP tubes for single-cell analysis. The remaining semen was put back into storage at -80 °C for later bulk measurements of semen. The semen samples were diluted with 1 mL of HEPES isotonic buffer for better centrifugal separation. It should be noted that we used the organic HEPES buffer instead of classic phosphate-buffered saline to minimize the presence of interfering elements, particularly P as the cell indicator. Sperm cells and seminal plasma were separated by mild centrifugation (550 *g* for 7 min). The supernatants were collected and stored at -20 °C for later bulk measurements of seminal plasma. The pellets were resuspended in HEPES buffer. The residual seminal plasma was removed by twice centrifugations (550 *g* for 7 min) and resuspended with 2 mL of HEPES buffer. The washed sperm cells were fixed by resuspending them with 2 mL of 4% PFA isotonic fixative (in HEPES buffer) for 15 min at room temperature. Due to the slight decrease in cell density after fixation, a relatively higher centrifugal force (750 *g* for 7 min) was used to separate the fixed sperm cells from the fixative. The fixed sperm cells were washed twice by centrifugation (750 *g* for 7 min) and resuspended in 2 mL of UPW, and then kept at 4 °C for short-term storage. Fixation and resuspension of sperm cells in UPW aims to remove interfering ions (mainly Na^+ and Cl^-) from the buffer, thus reducing interference with the detection of target elements in the cells and avoiding detector saturation. The fixed sperm cells in UPW retained morphological integrity (Fig. S2). Prior to scICP-TOF-MS analysis, cell number concentration was determined using a hemocytometer. The suspensions of fixed sperm cells were diluted with UPW to a final concentration of ~4×10^5 cells mL^{-1} for analysis. The treated sperm cells were demonstrated to be morphologically intact and free of matrix affecting scICP-TOF-MS assay.

The dispersed sperm cell suspensions were analyzed via an icpTOF 2R ICP-TOF-MS (TOFWERK AG; Thun, Switzerland) with operating parameters given in Table S1. Full mass spectra (from ^{7}Li to ^{238}U) were recorded with an extraction frequency of 21.7 kHz. Nebulizer efficiency was determined by the certified size method with 40 nm Au nanoparticles and dissolved Au solutions [3]. A series of concentrations of multi-element standard solutions were used to calibrate the element masses in single cells. A verification standard solution was measured between every ten samples for response correction.

Bulk measurement of semen and seminal plasma

The leftover semen and seminal plasma from the previous single-cell analysis were digested for bulk element analysis. Seminal plasma was further centrifuged (3000 *g* for 15 min) to remove residual sperm. The digestion and element measurement were performed in the same way for semen and seminal plasma, referring to the previous methods.[4-6] Samples of 0.2 mL of

semen or seminal plasma were taken into PP tubes, followed by the addition of 0.2 mL of HNO_3, and then left overnight. Then, 0.2 mL of H_2O_2 was added for an enhanced digestion of the organics. The mixed solution was heated in a water bath (90 °C for 3 hours) until completely clear and transparent. After self-cooling, the samples were diluted stepwise with 2% (*v*/*v*) HNO_3 to ensure an appropriate concentration range (0.1–200 μg L^{-1}) for all elements to be measured. An Agilent 7900 ICP-Q-MS (Agilent Technologies; Santa Clara, CA, USA) was used to determine the element concentrations (detailed operating parameters in Table S2). A series of concentrations of multi-element standard solutions (0.1–200 μg L^{-1}) were prepared for the determination of element concentrations by external standard method. In order to correct instrumental drift and matrix effects, a solution containing multiple internal standard elements (Li, Sc, Ge, Rh, In, Tb, Lu, and Bi) was simultaneously introduced into the ICP-MS with the sample through a three-way interface. Following the standard-sample-standard method, the multi-element standard solutions were measured repeatedly after every 25 samples. The blank control, sperm freezing medium, and HEPES buffer were treated and measured in the same way as the semen and seminal plasma samples. The element contents of these reagents were subtracted from that of semen and seminal plasma samples based on the amount added. Spiked pooled samples were also measured for quality control. The spiked recoveries for all the analyte elements ranged from 80.4% to 113.6%. All bulk measurements were repeated in triplicate.

Text S3 Data processing and analysis

Data processing for scICP-TOF-MS and bulk measurement.

TofDAQ Viewer (TOFWERK AG) and Tofware (TOFWERK AG) were used for mass recalibration of the recorded scICP-TOF-MS datasets considering mass drift. Cell event was identified via TOFpilot (TOFWERK AG) according to a recommended Poisson-based algorithm. The threshold value for cell events was determined by the following equation [7]:

$$Threhold = \mu + 3.29\sigma + 2.72 \quad (1)$$

where μ and σ are average signal intensity and the standard deviation of the signal intensity for the entire dataset of a sample, respectively. Data points above the threshold were picked out as cell events. Iteratively, the threshold was calculated based on the remaining data points, and the points above the threshold were picked out until no more cell events. The background intensity, from the average intensity of the dataset with cell events removed, was subtracted from the intensity of cell events. To prevent over- or under-estimation of the threshold value due to signal fluctuations during long-term measurement, every 1000 consecutive data points (obtained with a 3-second acquisition) served as an iterative calculation interval. ^{31}P was employed as an endogenous cell indicator to filter out false-positive events possibly caused by cell debris and other impurities (Fig. S2). The filtering processing was conducted by using a home-made Python script (see detail in https://github.com/st-tian/scICP-TOFMS.git). Absolute element masses in single cells were automatically calculated by TOFpilot with external standard curves. The limits of detection for element mass (LOD_{sc}; fg) were calculated with Equation (2) (derivation in Text S5):

$$LOD_{sc} = \frac{(3.29\sigma_{bkd} + 2.72)}{\alpha} \times \frac{\eta q t_d}{60} \times 10^6 \quad (2)$$

where σ_{bkd} is the standard deviation of the signal intensity for background signals (counts), α is the slope of the calibration curve (counts ng^{-1} mL), η is *the* nebulizer efficiency, q is the uptake flow rate (mL min^{-1}), and t_d is the dwell time (s). The data of the bulk measurements were acquired and processed with Mass Hunter software (Agilent Technologies). The limits of detection for bulk measurements (LOD_{bulk}; ng mL^{-1}) were calculated with Equation (3):

$$LOD_{bulk} = \frac{3\sigma_{bkd}}{\alpha} \quad (3)$$

Calculation of heterogeneity index.

Heterogeneity index (H), an established unified parameter to quantify the degree of heterogeneity in complex networks,[8] was employed to evaluate the heterogeneity of the element content in different sperm cells. H was calculated with Equation (4):

$$H = \frac{\sum_{i=1}^{N}\sum_{j=1}^{N}\left|m_i - m_j\right|}{2N^2\bar{m}} \quad (4)$$

where N is the number of detected cells in a certain sample, m_i and m_j are the masses of the element in any two cells, $\bar{m}$ is the average mass of the elements in the two cells. The value of H is in the range of 0–1. The closer H is to 1, the greater the variation in the contents of different cells (i.e., a higher degree of heterogeneity), and vice versa. It should be noted that, when only a few of some element events were identified in some samples, statistically significant H were unavailable (denoted with grey squares in the heatmap).

Statistical analysis.

The data from bulk measurements of the 150 samples were used for exploring the correlations between bulk element contents and semen quality. Excluding samples consumed in the pre-experiments, single-cell multi-element datasets of 119 of these samples were used for further statistical analysis. Conventional statistical analysis was performed using R program (version 4.1.3) and SPSS software (IBM; version 26). Normality and variance homogeneity of the experimental data were tested prior to the statistical analyses. Pearson test was used to analyze the correlations between element contents and semen quality parameters. Student *t*-test and Wilcoxon test were used to examine the difference between every two groups. Statistical significance was considered at the $p < 0.05$ level. The dataset recorded by scICP-TOF-MS is presented as a data matrix: thousands of cells are identified at different time points, each with multiple dimensions (i.e., multiple elements) of information (Fig. S1B). It is a challenge to explore element distribution patterns for such a large dataset. In some previous studies of nanoparticles, supervised machine learning algorithms were used to classify particles from different sources.[9, 10] Some particles from known sources were detected, and their element fingerprints were extracted. The sources of unknown samples can then be determined by comparing their element information with the fingerprints. However, for cell analysis, the cellular physicochemical properties are always obtained based on the statistics of randomly selected cells in the entire population. There is no quality information specific to a certain detected sperm cell herein. Therefore, it was unavailable to extract the element fingerprints of sperm cells with different qualities for training supervised machine learning models. Instead, unsupervised methods including dimension reduction and hierarchical clustering analysis were performed in this study. A machine learning-based Uniform Manifold Approximation and Projection (UMAP) method [11] was used to conduct dimension reduction of the dataset recorded by scICP-TOF-MS. This method facilitates the extraction of key features into two or three dimensions in tens to thousands of dimensions for subsequent data analysis. The key information for the elements of interest was extracted for each sample. Then, hierarchical clustering analysis was performed based on the dimension-reduced data,

with the elements of interest as clustering leaves. A correlation distance threshold of 1.5 was used to identify major clustering branches. The dimension reduction analysis and hierarchical clustering were performed in Python with the "umap" package and "scipy" package, respectively. Potential non-linear correlations of some important elements in the major clustering branches were further explored by a restricted cubic spline model based on piecewise linear regression. This data fitting process was performed in R program with the "rms" package. All the scripts used in this study are available in https://github.com/st-tian/scICP-TOFMS.git. The complete workflow of the data processing and analysis is illustrated in Fig. S1B.

Text S4 Bulk element contents of semen and seminal plasma and the correlations with semen quality

Fig. S3A shows the distribution of the element content in semen and seminal plasma, with the values close to those previously reported. [4, 6, 12, 13] Concentrations of Na, K, and P reached the mg mL^{-1} level. Concentrations of Ca, Mg, and Zn were lower up to the μg mL^{-1} level. Concentrations of the remaining elements were ng mL^{-1} or below. There were significant differences in the contents of P, Ca, Mg, Zn, Al, Rb, Cu, Sr, and Mn in semen and seminal plasma (Fig. S3A; $p < 0.01$ for paired-sample *t*-test or Wilcoxon test). Since semen contains sperm but seminal plasma does not, it was the element content in the sperm that caused these differences. In other words, at least, sperm cells contain a considerable amount of P, Ca, Mg, Zn, Al, Rb, Cu, Sr, and Mn.

Pearson tests revealed certain correlations between semen quality and the element contents in semen and seminal plasma (Fig. S3B). Elements with high concentrations, including Na, K, P, and Ca, exhibited less correlation with semen quality parameters. In semen, all measured elements except Na, Ca, and Al were significantly and positively correlated with sperm concentration and total sperm count ($p < 0.05$). In contrast, only Rb and Se showed such correlated relationships in seminal plasma. We consider that elements in sperm contributed to the more correlation relationships in semen, which highlights the significance of the direct element analysis of sperm cells. Zn, Rb, Fe, and Se in semen were positively correlated with the total motility (proportion of progressive and non-progressive sperm) and vitality (proportion of grade A and B sperm). Rb and Se were the few elements in seminal plasma that were positively correlated with sperm concentration, total sperm count, and total motility. Overall, the results herein agree well with those of previous studies. Previous studies have reported that low levels of K and Se can induce abnormal testosterone levels, thus affecting sperm production.[14, 15] Mg and Mn are essential elements for energy-related enzymes, and their deficiency can lead to poor sperm motility [16, 17]. There are many studies on Zn in human reproduction. Zn deficiency may lead to low sperm quality due to hormone deficiency, DNA damage, apoptosis, etc. [16]. As a non-essential element for life, Al in seminal plasma had a negative correlation with total motility ($r = -0.17$, $p < 0.05$) and a positive correlation with the percentage of grade D sperm ($r = 0.17$, $p < 0.05$) and immotile sperm ($r = 0.17$, $p < 0.05$), suggesting a negative effect of Al on semen quality.

Text S5 Derivation and discussion of the limits of detection (LODs)

LODs for scICP-TOF-MS

This derivation is based on the algorithm provided in the *Data processing and analysis* section.

The threshold value to identify cell events is determined with Equation (1):

$$Threhold = \mu + 3.29\sigma + 2.72 \tag{5}$$

When all events in a dataset have been picked out, the final threshold value is μ_{bkd}+3.27σ_{bkd}+2.72. Assuming that the minimum intensity of a certain event to be identified is I_{cell}. The minimum detectable event intensity is higher than the final threshold. The raw intensity ($I_{min\text{-}cell,\ raw}$) recorded by scICP-TOF-MS is attributed to a combination of the background signal intensity (I_{bkd}) and the event intensity ($I_{min\text{-}cell}$). Hence:

$$I_{min\text{-}cell,\ raw} = I_{bkd} + I_{min\text{-}cell} > \mu_{bkd} + 3.29\sigma_{bkd} + 2.72 \tag{6}$$

As described in our manuscript, the average intensity of the entire dataset with all events removed (μ_{bkd}) is considered as the background intensity (i.e., $I_{bkd} = \mu_{bkd}$). Hence:

$$I_{min\text{-}cell} > LOD_{intensity} = 3.29\sigma_{bkd} + 2.72 \tag{7}$$

Then, the minimum detectable intensity ($LOD_{intensity}$) can be converted into the corresponding mass (i.e., LOD_{mass}) with some measurement parameters and the external standard curve [18]:

$$LOD_{sc,\ mass} = \frac{\left(3.29\sigma_{bkd} + 2.72\right)}{\alpha} \times \frac{\eta q t_d}{60} \times 10^6 \tag{8}$$

where α is the slope of the calibration curve (counts ng^{-1} mL), η is *the* nebulizer efficiency, q is the uptake flow rate (mL min^{-1}), and t_d is the dwell time (s).

Since the matrix for scICP-TOF-MS is ultrapure water, after washing and dilution procedures, the background noise is close to the signal intensity of the blank control. Consequently, σ_{bkd} can also be replaced with σ_{blk} for calculation:

$$LOD_{sc,\ mass} = \frac{\left(3.29\sigma_{blk} + 2.72\right)}{\alpha} \times \frac{\eta q t_d}{60} \times 10^6 \tag{9}$$

In this study, the *LOD*s were calculated based on the background signals with all the cell events removed following Equation (8) (i.e., LOD_{bkd}; Table S3). Besides, the *LOD*s based on the blank controls (LOD_{blk}) were also estimated for validation. Overall, LOD_{bkd} was higher LOD_{blk}. The higher LOD_{bkd} may be attributed to the following reasons: (1) despite washing many times, residual element ions in the bio-fluid (i.e., seminal plasma), buffer, and fixative solution were inevitable; (2) some events with particularly low signal intensity may be considered as background, somewhat raising the average level of the baseline; and (3) some of the elements in the cells may be partially lost to the extracellular medium after fixation, resulting in decreased content in sperm cells and elevated $LOD_{sc,\ mass}$. Further exploration is recommended to reduce $LOD_{sc,\ mass}$ in the future study. First, the cell fixation procedure can possibly be further optimized to minimize element loss and thus improve the signal-to-noise

ratio, which may be important for free-state dominated elements. Besides, ICP-TOF-MS instruments with higher mass resolution and sensitivity are urgently needed for future tests.

LODs for bulk analysis

For bulk element measurement, the minimum quantifiable signal intensity is generally $\mu_{bkd}+3\sigma_{bkd}$. Similarly, the raw intensity ($I_{min,\,raw}$) is attributed to a combination of the background signal intensity (I_{bkd}) and the sample intensity (I_{min}). Hence:

$$I_{min,\,raw} = I_{bkd} + I_{min} > \mu_{bkd} + 3\sigma_{bkd} \tag{10}$$

Then:

$$I_{min} > LOD_{intensity} = 3\sigma_{bkd} \text{ or } 3\sigma_{blk} \tag{11}$$

According to the external standard curve：

$$LOD_{bulk,\,concentration} = \frac{3\sigma_{bkd}}{\alpha} \text{ or } \frac{3\sigma_{blk}}{\alpha} \tag{12}$$

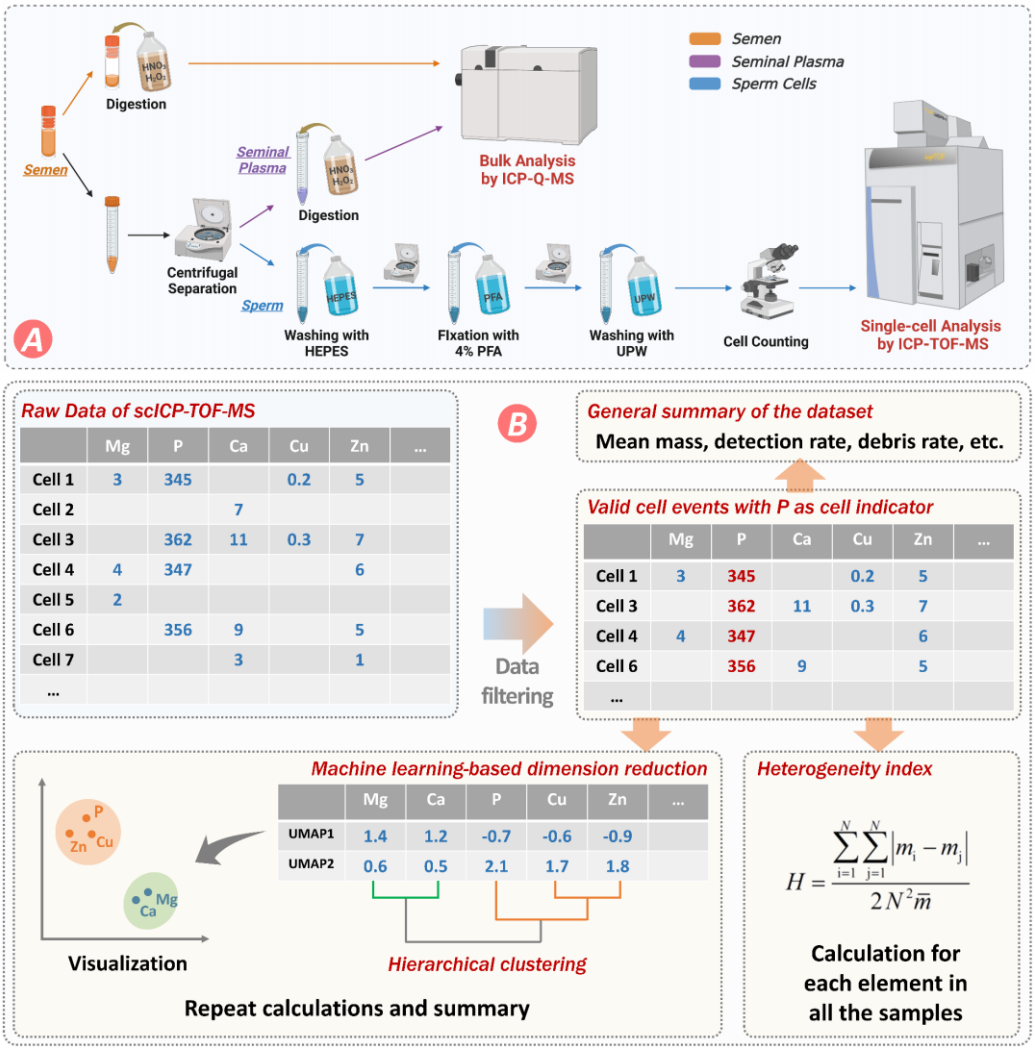

Figure S1 (A) Workflow of the multi-element analyses of semen, seminal plasma, and sperm cells. First, a portion of the semen was taken out for the analysis of seminal plasma and sperm cells. Seminal plasma and sperm cells were separated by mild centrifugation. Then, the seminal plasma and the remaining semen were digested with acid and measured via an ICP-Q-MS. Sperm cells were washed, fixed, counted, and diluted for scICP-TOF-MS analysis. (B) Workflow of the data processing and analysis of the large dataset recorded by scICP-TOF-MS. First, false-positive cell events were filtered out with P signals as the cell indicator. Some general parameters, such as mean element masses, element detection rates, and cell debris rates, were summarized. Heterogeneity indexes for each element in all the samples were calculated to evaluate the variations of element contents in different cells. Afterwards, dimension reduction analysis was performed to extract key features of the element distribution in single cells. The processed data were visualized and hierarchically clustered to explore the cellular element distribution pattern.

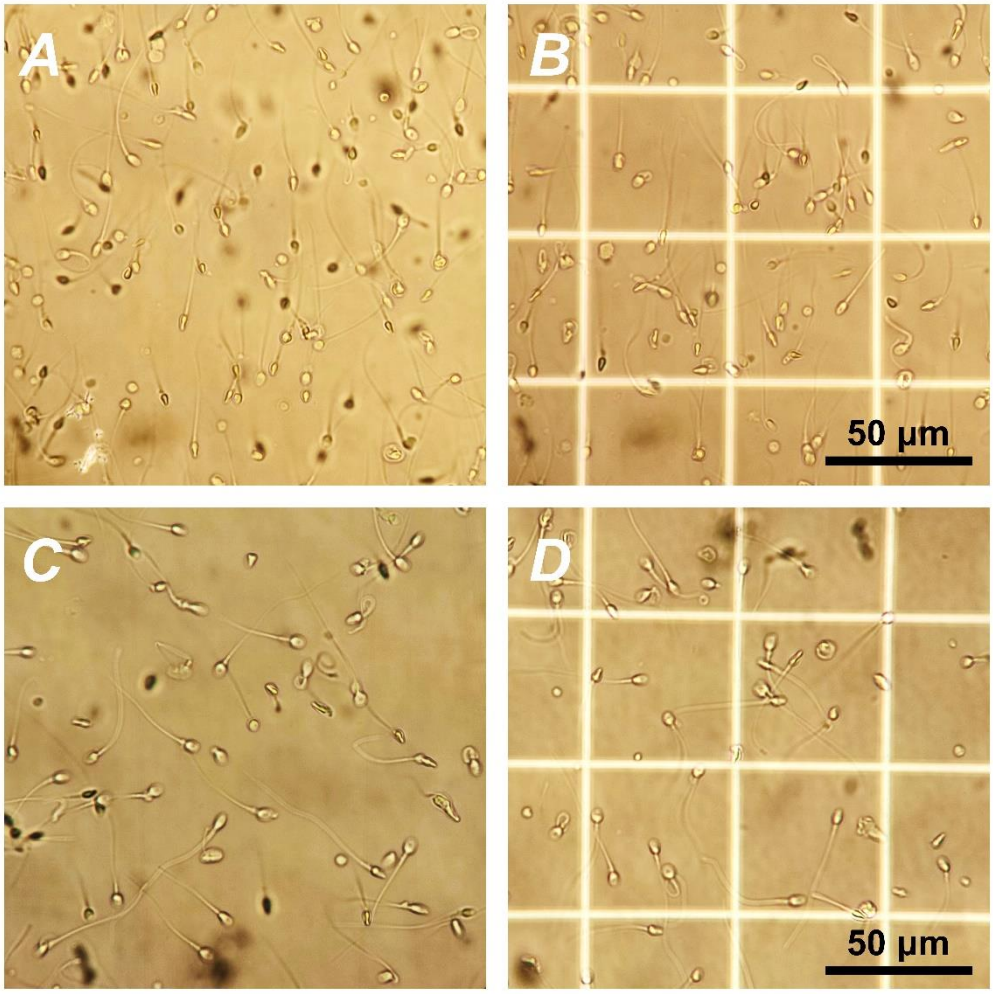

Figure S2 Microscopic images of the sperm cells (400×). (A) and (B) show the frozen-thawed sperm cells. It was demonstrated that the sperm cells maintained their full morphology and good motility. (C) and (D) show the fixed sperm cells. The fixed cells in ultrapure water were still morphologically intact.

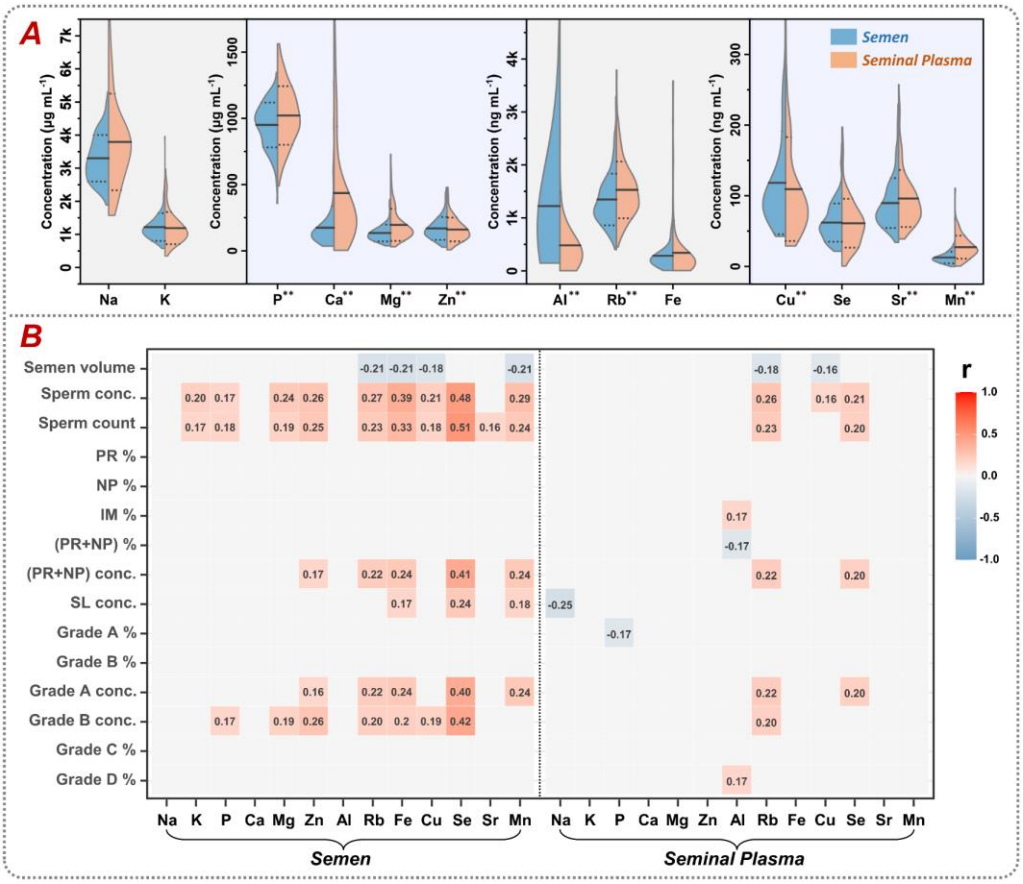

Figure S3 (A) Distribution of bulk element concentrations in semen (blue) and seminal plasma (orange). The superscripts (**) of the elements denote significant differences ($p < 0.01$) in the content of the elements between semen and seminal plasma. The data were measured via Agilent 7900 ICP-Q-MS. Statistical tests were performed using paired-sample t-test or Wilcoxon test. (B) Pearson correlations between semen quality parameters and element content in semen and seminal plasma. The color blocks marked with numbers indicate significant correlations ($p < 0.05$), with the numbers denoting the Pearson correlation coefficients (r). Abbreviations: conc., concentration; %, percentage; PR, progressive (motility); NP, non-progressive (motility); IM, immotility; SL, straight-line (motility).

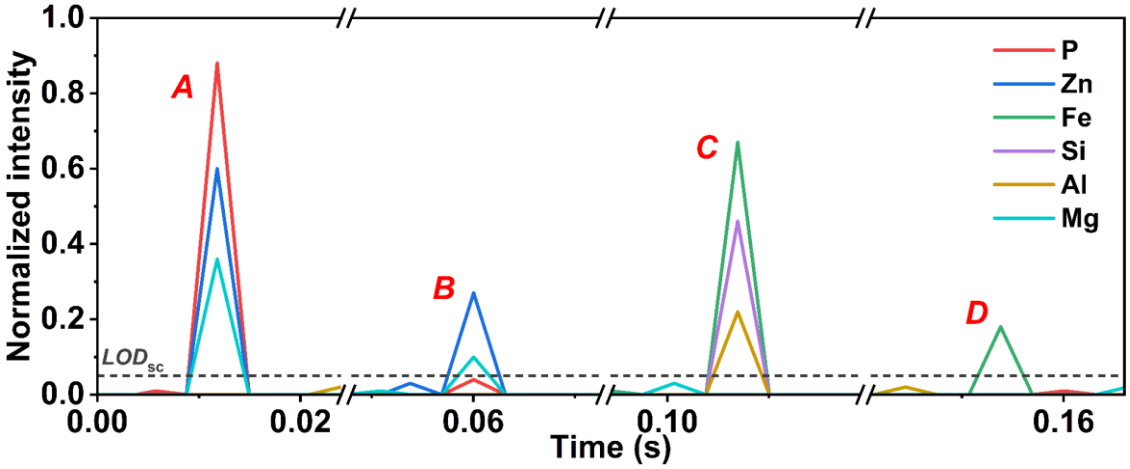

Figure S4 Typical examples of the peak signals recorded by single-cell ICP-TOF-MS. Peak A is supposed to be a cell event due to the detection of both life-essential elements and the cell indicator element P with a high intensity. Whereas peaks B, C, and D are more likely to be false-positive cell events. Although some life-essential elements were detected in peak B, the intensities are low, and no P signals were detected. Accordingly, peak B is probably generated from cell debris. Peak C shows the signals of some inorganic elements with high intensities, probably attributed to fine particulate matter in the matrix. Peak D is more likely attributed to signal fluctuation as only one element with very low intensity was detected.

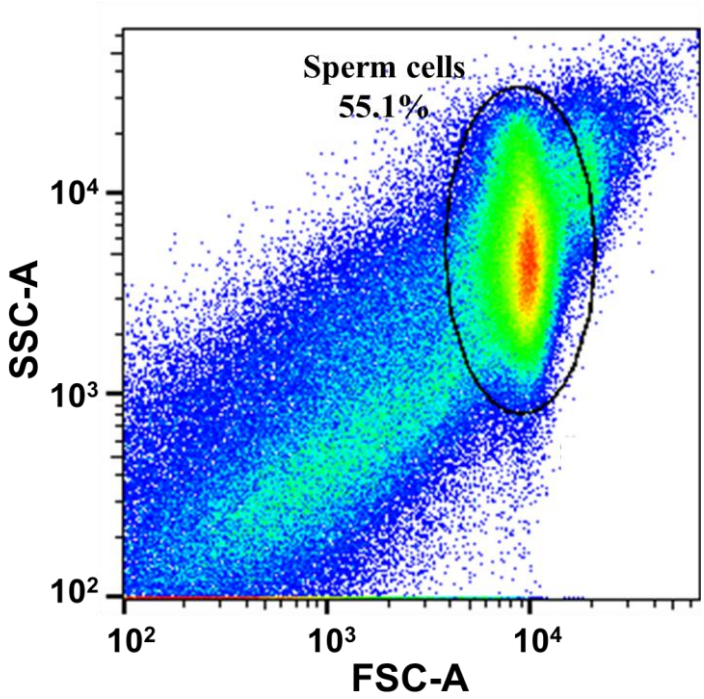

Figure S5 Scatter plots of the fixed and washed sperm cells counted by flow cytometry. Side scatter area (SSC-A) and forward scatter area (FSC-A) were used to gate sperm cells.[19]

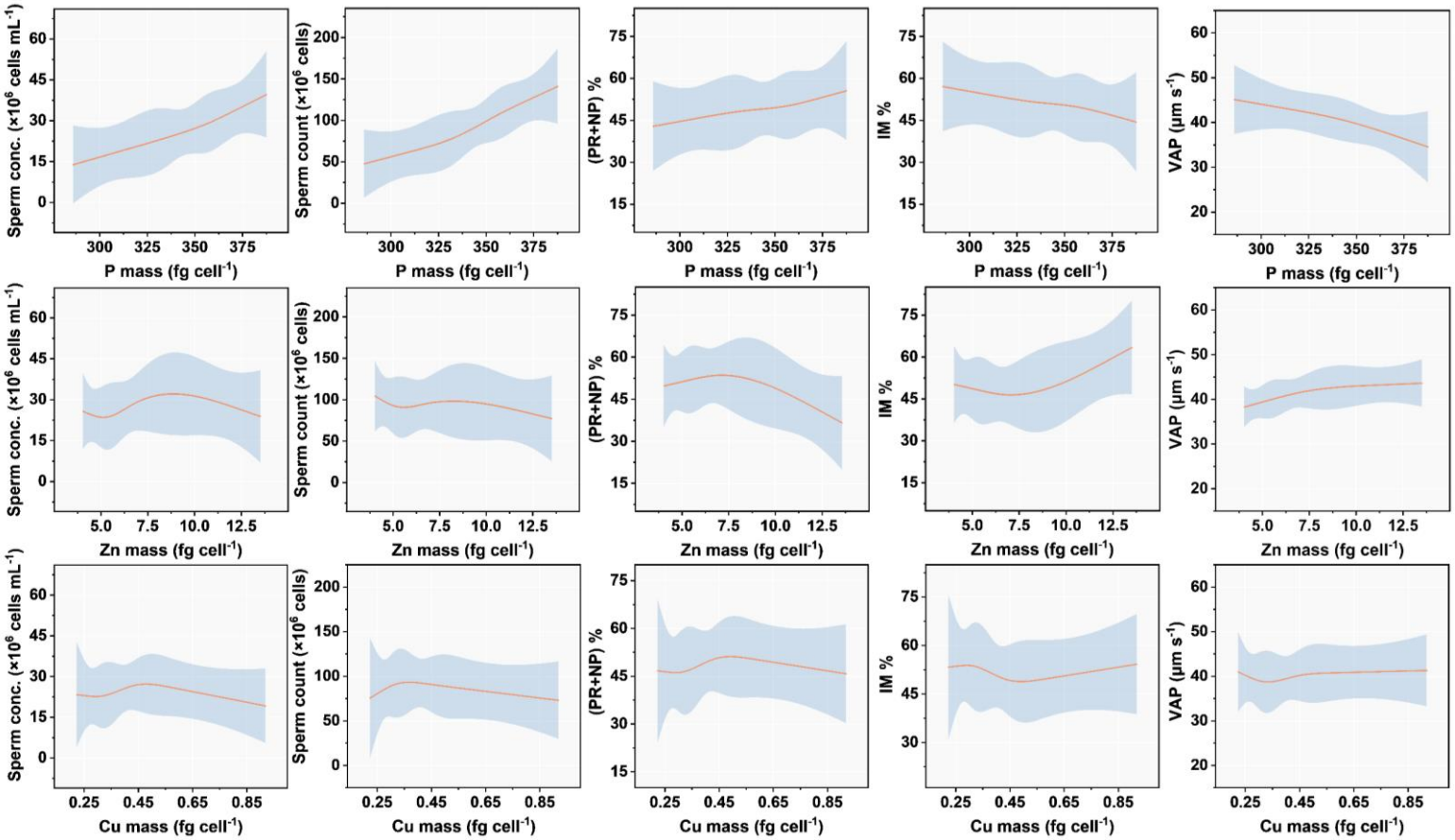

Figure S6 Potential correlations between semen quality parameters and P, Zn, and Cu contents in single cells. The orange lines represent the predicted semen quality parameters at different cellular element mass, and the blue intervals denote the 95% confidence intervals. The predictions were performed with a restricted cubic spline model based on the measured single-cell data (see details in https://github.com/st-tian/scICP-TOFMS.git). Abbreviations: conc., concentration; %, percentage; PR, progressive (motility); NP, non-progressive (motility); IM, immotility; VAP, average path velocity.

Table S1 Operating parameters for icpTOF 2R ICP-TOF-MS

Parameter	Conditions
Sample uptake rate (mL min^{-1})	0.400
ICP RF power (W)	1550
Nebulizer gas flow (L min^{-1})	1.06
Auxiliary gas flow (L min^{-1})	0.80
Spectrum acquisition frequency (kHz)	21.7
Dwell time (s)	0.003
Notch *m*/*z*	31.5, 35.7, 40.3, 80.0

Table S2 Operating parameters for Agilent 7900 ICP-Q-MS

Parameter	Conditions	
Mode	Standard mode	Time-resolved mode
Sample uptake rate (mL min^{-1})	0.346	0.346
ICP RF power (W)	1550	1550
Auxiliary gas flow (L min^{-1})	0.80	0.80
Nebulizer gas flow (L min^{-1})	1.04	1.25
Integration/dwell time (s)	0.100	0.003
Helium gas flow (mL min^{-1})	5	Not used

Table S3 Estimated element masses in single sperm cells and the limits of detection for element mass in single-cell ICP-TOF-MS analysis.

	Estimated element mass (fg cell^{-1}) [a]	$LOD_{sc,\ mass}$ (fg cell^{-1})
Na	/	50.14 ± 39.97
Mg	5.15 ± 0.48	2.59 ± 0.99
Al	5.65 ± 2.68	0.56 ± 0.06
P	614.78 ± 113	126.46 ± 17.16
K	~8.17	146.90 ± 16.38
Ca	14.64 ± 8.04	8.82 ± 1.15
Mn	0.12 ± 0.02	0.10 ± 0.02
Fe	6.33 ± 2.13	14.3 ± 3.6
Ni	0.06 ± 0.04 (~0.04 [5]) [b]	0.60 ± 0.04
Cu	0.22 ± 0.06 (0.55 [20]) [b]	0.12 ± 0.05
Zn	22.59 ± 11.20 (39.90 [21]) [b]	3.64 ± 1.38
Se	0.31 ± 0.09 (0.25 ± 0.14 [22]) [b]	299.28 ± 9.92
Rb	0.05 ± 0.01	0.07 ± 0.01
Ba	0.12 ± 0.06	0.33 ± 0.11

Note:

[a] In this study, samples of 1 mL semen were randomly taken for estimation. First, the semen samples were washed and centrifuged following the methods described in the main text to obtain the sperm cells. The number of sperm cells was counted with a hemocytometer. Then, the cells were dried at 80 °C. The digestion and ICP-MS measurements followed the methods for the bulk measurement of semen and seminal plasma. The element mass of single sperm cells (m_S) was calculated with the following equation:

$$m_S = \frac{m_T}{n} \tag{13}$$

where m_T is the total mass, and n is the total cell count. Noted that to minimize cell lysis, we did not use ultrapure water but only HEPES buffer (containing 0.9% *w*/*v* NaCl) for washing. Consequently, we considered that the Na mass in single sperm cells was particularly unreliable due to the NaCl residues and therefore not provided in this table.

[b] Data in brackets are from previous studies.

Reference

1. W. H. Organization, *WHO Laboratory manual for the examination and processing of human semen*, World Health Organization, 5th edn., 2010.
2. U. Marzec-Wróblewska, P. Kamiński, P. Łakota, M. Szymański, K. Wasilow, G. Ludwikowski, L. Jerzak, T. Stuczyński, A. Woźniak and A. Buciński, *Biol. Trace Elem. Res.*, 2019, **188**, 251–260.
3. H. E. Pace, N. J. Rogers, C. Jarolimek, V. A. Coleman, C. P. Higgins and J. F. Ranville, *Anal. Chem.*, 2011, **83**, 9361–9369.
4. A. Zafar, S. A. Eqani, N. Bostan, A. Cincinelli, F. Tahir, S. T. Shah, A. Hussain, A. Alamdar, Q. Huang, S. Peng and H. Shen, *Environ. Geochem. Health*, 2015, **37**, 515–527.
5. A. E. Calogero, M. Fiore, F. Giacone, M. Altomare, P. Asero, C. Ledda, G. Romeo, L. M. Mongioì, C. Copat, M. Giuffrida, E. Vicari, S. Sciacca and M. Ferrante, *Ecotoxicol. Environ. Saf.*, 2021, **215**, 112165.
6. M. Katayama, S. Kaneko, K. Takamatsu, T. Tsukimura and T. Togawa, *J. Mol. Biomarkers Diagn.*, 2013, **4**, 1000147.
7. M. Tanner, *J. Anal. At. Spectrom.*, 2010, **25**, 405–407.
8. H.-B. Hu and X.-F. Wang, *Phys. A*, 2008, **387**, 3769–3780.
9. A. Praetorius, A. Gundlach-Graham, E. Goldberg, W. Fabienke, J. Navratilova, A. Gondikas, R. Kaegi, D. Günther, T. Hofmann and F. von der Kammer, *Environ. Sci.: Nano*, 2017, **4**, 307–314.
10. G. D. Bland, M. Battifarano, A. E. Pradas Del Real, G. Sarret and G. V. Lowry, *Environ. Sci. Technol.*, 2022, **56**, 2990–3001.
11. L. McInnes, J. Healy and J. Melville, *arXiv*, 2018, **1802.03426**, 1–63.
12. P. Li, Y. Zhong, X. Jiang, C. Wang, Z. Zuo and A. Sha, *Biol. Trace Elem. Res.*, 2012, **148**, 1–6.
13. M. I. Camejo, L. Abdala, G. Vivas-Acevedo, R. Lozano-Hernandez, M. Angeli-Greaves and E. D. Greaves, *Biol. Trace Elem. Res.*, 2011, **143**, 1247–1254.
14. A.-W. R. Hamad, H. I. Al-Daghistani, W. D. Shquirat, M. Abdel-Dayem and M. Al-Swaifi, *Biochem. Pharmacol.*, 2014, **03**, 1000141.
15. O. Akinloye, A. O. Arowojolu, O. B. Shittu, C. A. Adejuwon and B. Osotimehin, *Biol. Trace Elem. Res.*, 2005, **104**, 9-18.
16. M. Mirnamniha, F. Faroughi, E. Tahmasbpour, P. Ebrahimi and A. Beigi Harchegani, *Rev. Environ. Health*, 2019, **34**, 339–348.
17. R. S. Cheema, A. K. Bansal and G. S. Bilaspuri, *Oxid. Med. Cell. Longevity*, 2009, **2**, 152–159.
18. X. Tian, H. Jiang, L. Hu, M. Wang, W. Cui, J. Shi, G. Liu, Y. Yin, Y. Cai and G. Jiang, *TrAC, Trends Anal. Chem.*, 2022, **157**, 116746.
19. S. J. Gunderson, L. C. Puga Molina, N. Spies, P. A. Balestrini, M. G. Buffone, E. S. Jungheim, J. Riley and C. M. Santi, *Fertil. Steril.*, 2021, **115**, 930–939.
20. D. Xu, G. Yang and J. Cao, *Spectrom. Spectral Anal. (in Chinese)*, 1996, **16**, 87–90.
21. R. Henkel, J. Bittner, R. Weber, F. Huther and W. Miska, *Fertil. Steril.*, 1999, **71**, 1138–1143.
22. D. Behne, H. Gessner, G. Wolters and J. Brotherton, *Int J Androl*, 1988, **11**, 415–423.